0013-7227/08/$15.00/0
Printed in U.S.A.

Endocrinology 149(5):2620–2627
Copyright © 2008 by The Endocrine Society
doi: 10.1210/en.2007-1563

Low Doses of Insulin-Like Growth Factor-I Induce Mitochondrial Protection in Aging Rats

Juan E. Puche, María García-Fernández, Jordi Muntané, José Rioja, Salvador González-Barón, and Inma Castilla Cortazar

Department of Medical Physiology (J.E.P., I.C.C.), School of Medicine, University Universidad San Pablo-CEU, 28668 Madrid, Spain; Department of Medical Physiology (J.E.P., M.G.-F., J.R., S.G.-B., I.C.C.), School of Medicine, University of Málaga, 29071 Málaga, Spain; and Department of Internal Medicine (J.M.), Liver Unit, University of Córdoba, 14080 Córdoba, Spain

Serum IGF-I levels decline with age. We have recently reported that in aging rats the exogenous administration of IGF-I restores IGF-I circulating levels and age related-changes, improving glucose and lipid metabolisms, increasing testosterone levels and serum total antioxidant capability, and reducing oxidative damage in the brain and liver associated with a normalization of antioxidant enzyme activities. Understanding that mitochondria are one of the most important cellular targets of IGF-I, the aims of this study were to characterize mitochondrial dysfunction and study the effect of IGF-I therapy on mitochondria, leading to cellular protection in the following experimental groups: young controls, untreated old rats, and aging rats treated with IGF-I. Compared with young controls, untreated aging rats showed an increase of oxidative damage in isolated mitochondria with a mitochondrial dysfunction characterized by: depletion of membrane potential with increased proton leak rates and intramitochondrial free radical production, and a significant reduction of ATPase and complex IV activities. In addition, mitochondrial respiration from untreated aging rats was atractyloside insensitive, suggesting that the adenine nucleotide translocator was uncoupled. The adenine nucleotide translocator has been shown to be one of the most sensitive locations for pore opening. Accordingly, untreated aging rats showed a significant overexpression of the active fragment of caspases 3 and 9. IGF-I therapy corrected these parameters of mitochondrial dysfunction and reduced caspase activation. In conclusion, these results show that the cytoprotective effect of IGF-I is closely related to a mitochondrial protection, leading to reduce free radical production, oxidative damage, and apoptosis, and to increased ATP production. (*Endocrinology* 149: 2620–2627, 2008)

AGING IS CHARACTERIZED by a significant decline of metabolic and hormonal functions that often contributes to the onset of severe age-associated pathologies. IGF-I is an anabolic hormone produced mainly in the liver in response to GH stimulation (1). Circulating IGF-I serum levels decline by more than 50% in healthy older adults (2, 3).

We have recently reported that the exogenous administration of low doses of IGF-I restores IGF-I circulating levels and some age-related changes, improving glucose and lipid metabolisms, increasing testosterone levels and serum total antioxidant capability, and reducing oxidative damage in the brain and liver associated with a normalization of antioxidant enzyme activities and mitochondrial membrane potential (MMP) (4). From these results we suggested that aging seems to be an unrecognized condition of "IGF-I deficiency." The best-known condition of "IGF-I deficiency" is Laron's dwarfism (5), characterized by an absence of GH receptors in the liver. Another condition of IGF-I deficiency is liver cirrhosis. In cirrhosis the reduction of receptors for GH in hepatocytes and the diminished ability of the hepatic parenchyma to synthesize cause a progressive decrease in serum IGF-I levels (6). We have shown previously that short courses of treatment with low doses of IGF-I in rats with carbon tetrachloride-induced cirrhosis induced many systemic beneficial effects, and showed hepatoprotective and antioxidant properties, including mitochondrial protection (7–12).

The reported cytoprotective (neuroprotective and hepatoprotective) activity of IGF-I in aging rats (4) could also be related to mechanisms of mitochondrial protection. In fact, in the study by García-Fernández *et al*. (4), untreated aging animals showed a depletion of MMP with a significant reduction of ATP synthesis, which IGF-I replacement therapy was able to correct to the normal values of young rats.

Mitochondria are particularly sensitive to damage induced by reactive oxygen species (ROS) in the pathogenesis of disease and aging (13, 14). Normal mitochondrial function is a critical place in maintaining cellular homeostasis because mitochondria produce ATP and are the major intracellular source of free radicals. Cellular dysfunctions induced by intracellular or extracellular insults converge on mitochondria and induce a sudden increase in permeability on the inner mitochondrial membrane, the so-called mitochondrial membrane permeability transition (MMPT). MMPT is caused by the opening of pores in the inner mitochondrial

First Published Online February 14, 2008

Abbreviations: ANT, Adenine nucleotide translocator; Atr, atractyloside; AU, arbitrary unit; EC, Enzyme Commission of the International Union of Biochemistry; FL, fluorescence; GRD, glutathione reductase; GSHPx, glutathione peroxidase; LOOH, lipid hydroperoxide; MMP, mitochondrial membrane potential; MMPT, mitochondrial membrane permeability transition; ns, not significant; O, untreated old rat; O + IGF-I, aging rats treated with IGF-I; RCR, respiratory control ratio; ROS, reactive oxygen species; SOD, superoxide dismutase; TAS, total antioxidant status; yCO, young healthy control.

***Endocrinology* is published monthly by The Endocrine Society (http://www.endo-society.org), the foremost professional society serving the endocrine community.**

Downloaded from endo.endojournals.org at Univ San Pablo Biblioteca De Ciencias on March 10, 2009

membrane, matrix swelling, and outer membrane rupture. The MMPT is an endpoint to initiate cell death because the pore opening together with the release of mitochondrial cytochrome *c* activates the apoptotic pathway of caspases. Cellular targets of the effector caspases include endonucleases and cytoskeletal proteins (15). Adenine nucleotide translocator (ANT) catalyzes the exchange of ATP and ADP between the mitochondria and the cytosol. It has also been shown to be a significant mediator of the basal proton leak in mitochondria and one of the most sensitive points for pore opening (16).

Understanding that mitochondria are one of the most important cellular targets of IGF-I (4, 11, 12), the aims of the present study were to characterize the mitochondrial dysfunction in aging rats and to investigate the effect of IGF-I therapy on damaged mitochondria leading to cellular protection. With these aims, we have extended this study to analyze the effect of IGF-I on mitochondrial function parameters, such as MMP, oxygen consumption, intramitochondrial free radical production, proton leak rates, cytochrome *c* oxidase and ATPase activities, inhibition of ANT by atractyloside (Atr), intramitochondrial oxidative damage, and intramitochondrial antioxidant enzyme activities (16–23). All of these were assessed in isolated hepatic mitochondria, and caspase 3 activation and caspase 9 were determined in liver homogenates in the following experimental groups: young healthy controls (yCO) (17 wk old, n = 6); untreated old rats (O group) (103 wk old, n = 6); and aging rats (103 wk old) treated with IGF-I (O + IGF-I) during 1 month (2.25 μg IGF-I/100 g body $wt^{-1}{\cdot}d^{-1}$, n = 6).

Materials and Methods

Animals and experimental design

All experimental procedures were performed in conformity with *The Guiding Principles for Research Involving Animals* (24). Healthy male Wistar rats, 17 wk old, were used in this protocol as young controls (yCO, n = 6), and healthy male Wistar rats of 103 wk old were randomly assigned to receive either saline (group O, n = 6) or recombinant human IGF-I (Chiron Co., Emeryville, CA) (2.25 μg IGF-I/100 g body $wt^{-1}{\cdot}d^{-1}$ in two divided doses) (group O + IGF, n = 6) sc for 30 d.

Both food (standard semipurified diet for rodents; B.K. Universal, Sant Vicent del Horts, Spain) and water were given *ad libitum*. Rats were housed in cages placed in a room with a 12-h light, 12-h dark cycle, and constant humidity and temperature (20 C).

In the morning of the 31st day, rats were killed by decapitation, and the liver was dissected. Fresh liver was used to isolate mitochondria and to perform mitochondrial function tests using flow cytometry (4, 11). Samples were obtained simultaneously from young, old-untreated rats, and old rats treated with IGF-I to have paired data.

Isolation of liver mitochondria

Liver mitochondrial fraction was prepared according to the method described by Schneider and Hogeboom with modifications (11, 17, 42). Liver samples were homogenized (1:10 wt/vol) in an ice-cold isolation buffer containing sucrose 0.25 M and 0.1% BSA buffered (pH 7.4) with Tris-HCl 10 mM, and the isolation medium was identical without BSA or EDTA. The protein concentration was measured using the Biuret method. The homogenate was centrifuged at 800 × *g* for 10 min. The resulting supernatant was centrifuged at 8500 × *g* for 10 min. The supernatant was discarded, and the pellet was diluted in cold isolation buffer and centrifuged at 8500 × *g* for 10 min three times. The final mitochondria pellet was resuspended in a minimal volume, and aliquots were stored at −80 C until use in enzyme assays. All procedures were conducted at 4 C.

Unless otherwise indicated, the standard incubation medium had the following composition: 100 mM NaCl, 5 mM sodium-potassium phosphate buffer (pH 7.4), 10 mM Tris-HCl buffer (pH 7.4), and 10 mM $MgCl_2$. The respiratory substrates used were 5 mM potassium glutamate plus 2.5 mM potassium malate and 5.0 mM potassium succinate plus 4 μM rotenone.

Oxygen consumption

Oxygen consumption was measured using a Clark-type electrode (Hansatech Instruments Ltd., using software OXIGRAPH version 1.10; Norfolk, UK) in a 2-ml glass chamber equipped with magnetic stirring. The reaction was started by the addition of 6 mg mitochondrial protein to 2 ml standard medium containing rotenone 5 μM, oligomycin 1.3 mM, nigericin 100 pmol/mg protein, succinate 10 mM, ADP 200 μM, and glutamate/malate 5/2.5 mM. Finally, it was stabilized for 1 min at 30 C. Respiration rates are given in nAtom-gram oxygen/mg·min. Phosphorylating respiration (state 3) was initiated by addition of 200 nmol ADP/mg protein. Phosphorylation efficiency (ADP/O ratio) was calculated from the added amount of ADP and total amount of oxygen consumed during state 3. The state 4 is obtained with all substrates but ADP.

The ratio between state 3 rate and state 4 rate is called the respiratory control ratio (RCR), and indicates the tightness of the coupling between respiration and phosphorylation. With isolated mitochondria the coupling is not perfect, probably as a result of mechanical damage during the isolation procedure. Typical RCR values range from three to 10, varying with the substrate and the quality of the preparation. Coupling is thought to be better *in vivo* but may still not achieve 100%.

Flow cytometry analysis

Gated mitochondrial population was chosen by flow cytometry, based on forward scatter and side scatter within mitochondria samples, after obtaining one clear mitochondria population.

Mitochondrial transmembrane electrical potential. MMP ($\Delta\psi$) was measured by the lipophilic cationic fluorescent probe Rh-123 (Molecular Probes Inc., Eugene, OR), a fluorescent derivative of uncharged dihydroRh-123, according to previous studies (4, 11, 17). A mitochondrial suspension (50 μg/ml) was incubated with the same respiratory substrates used in oxygen uptake for 1 min at room temperature, and after adding Rh-123 (260 nM) and incubating it for another minute. After incubation, suspensions were immediately analyzed by flow cytometry. The values of the fluorescence (FL) substrates were normalized to the value obtained with the uncoupler carbonylcyamide-m-chlorophenylhydrazone.

Rate of intramitochondrial free radical generation. The rate of ROS generation from mitochondria was measured after the formation of Rh-123 using the cytometry method performed by O'Connor (17) with a small modification. A mitochondrial suspension (100 μg/ml) was incubated with 0.82 nM dihydro Rh-123 and 7 U/ml horseradish peroxidase for 5 min at room temperature. The values of the FL substrates were normalized to the value obtained without peroxidase and adding the uncoupler CCCP. H_2O_2 (1 mM) was used with the positive control.

After incubation, the suspensions were immediately analyzed. Gated mitochondrial population was chosen by flow cytometry, based on forward scatter and side scatter within mitochondria samples.

Cytofluorometric analysis was performed using a flow cytometer EPICS XL (Beckman Coulter, Inc., Fullerton, CA) equipped with a single 488-nm argon laser (15 mW). Green FL was detected with a wide-band filter for Rh-123 centered in 525 ± 20 nm (FL1). A standard cytogram based on the measurement of right angle scatter *vs.* forward angle scatter was defined to eliminate cellular debris and aggregates. A minimum of 10,000 mitochondria per sample was acquired in list mode and analyzed with System II version 3.0 software (Beckman Coulter).

Activities of mitochondrial complexes

Mitochondrial suspensions were thawed and diluted with potassium phosphate. Activities of the respiratory chain enzymes were measured at 37 C in Cobas Mira (ABXMicro, Mannheim, Germany).

Downloaded from endo.endojournals.org at Univ San Pablo Biblioteca De Ciencias on March 10, 2009

Measurements of cytochrome oxidase activity. Cytochrome oxidase activity was measured according to the method described by Cortese *et al.* (23). Mitochondria were resuspended in the medium containing (in mM) 220 mannitol, 70 sucrose, 2.5 K_2HPO_4, 2.5 $MgCl_2$, and 0.5 EDTA. Antimycin A was then added to block mitochondrial respiration through complex III. Reaction was started by adding ascorbate/*N*,*N*,*N*′,*N*′-tetramethyl-*p*-phenylenediamine as an electron donor.

Complex V, ATPase (EC 3.6.1.34.) The activity was assayed by coupling the reaction to the pyruvate kinase and lactate dehydrogenase systems, and measuring reduced nicotinamide adenine dinucleotide (NADH) oxidation at 340 nm. The assay system contained Tris-HCl buffer 65 mM (pH 7.5), sucrose 300 mM, $MgCl_2$ 4.75 mM, ATP 4 mM, NADH 0.4 mM, phosphoenolpyruvate 0.6 mM, potassium cyanide 5 mM, pyruvate kinase 700 U/ml, and lactate dehydrogenase 1000 U/ml.

Assessment of "proton leak": the relationship between respiration rate and MMP ($\Delta\psi$)

Mitochondrial proton leak was calculated from respiration rates and MMP expressing the ratio of protons for each oxygen atom consumed (18–21). The rate of proton leak across the inner mitochondrial membrane is a function of the driving force (membrane potential) and increases disproportionately with membrane potential.

Titration of membrane potential and state 4 oxygen consumption by respiratory inhibitors were performed simultaneously in separate vessels at 30 C. Nigericin was added to collapse the pH difference across the mitochondrial inner membrane and, thus, $\Delta\psi$ had the value of the proton motive force (Δp). Reactions were started by the addition of 3 mg mitochondrial protein/ml standard medium containing also 3 mM rotenone, 1.3 mM oligomycin, nigericin (100 pmol/mg protein), and 5 mM succinate. The addition of inhibitors was begun when the maximum value of the potential became stable (after ~2–3 min). When succinate was used as the substrate, the titration was performed with malonate (K/salt) from 0–13 mM; at the end of each membrane potential trace, the zero point was determined by addition of CCCP 1 mM. Rates of respiration during the titration with inhibitors were measured with a Clarke-type oxygen electrode, and membrane potential with a flow cytometer simultaneously with the measurements of membrane potential.

Inhibition of ANT by Atr

To establish the optimal concentration of Atr (Calbiochem-Novabiochem, San Diego, CA) needed for ANT inhibition, the efficiency of Atr was first examined in its classical role, *i.e.* for its ability to inhibit oxidative phosphorylation. For analysis, increasing Atr concentrations (50–200 pmol/mg mitochondrial protein) were used until complete inhibition of oxygen consumption was obtained (22).

Oxidative damage and total antioxidant status (TAS) in isolated mitochondria

Lipid hydroperoxides (LOOHs) were assessed in isolated mitochondria as previously described by Arab and Steghens (25), and adapted for Cobas Mira (600-nm wavelength) and mitochondria suspensions. Briefly, orange xylenol (180 μl–167 μM) was added to 25 μl sample. The first optic reading was obtained before the addition of iron gluconate (45 μl-833 μM). LOOH was calculated using a standard curve of tert-butyl hydroperoxide, and LOOH levels were expressed as nmol/mg mitochondrial protein. Intraassay and interassay coefficients were 3 and 8%, respectively.

TAS, as total enzymatic and nonenzymatic antioxidant capability, was evaluated in isolated mitochondria by a colorimetric assay (Randox Laboratories Ltd., Ardmore, Crumlin, UK) using the following principle: 2,2′-azino-di-('3-ethylbenzthiazoline sulfonate) was incubated with a peroxidase (metmyoglobin) and H_2O_2 to produce the radical cation 2,2′-azino-di-('3-ethylbenzthiazoline sulfonate)$^{\cdot+}$. This has a relatively stable blue-green color, which is measured at 600 nm. Antioxidants in the added sample cause suppression of this color production to a degree that is proportional to their concentration (26, 27).

Activities of antioxidant enzymes in isolated mitochondria

Activities of superoxide dismutase (SOD) (EC 1. 15. 1. 1.), glutathione reductase (GRD) (EC 1.6.4.2), and glutathione peroxidase (GSHPx) (EC 1.11.1.9.) were measured in liver mitochondria. Antioxidant activities were determined at 37 C using a commercial kit (Ransod; Randox Laboratories) and an autoanalyzer (Cobas Mira; Roche Diagnostic System, Basel, Switzerland).

Western blots for caspase 3 and caspase 9 in liver homogenates

Frozen livers (1 g) were homogenized (Ultra-turrax T25; Janke & Kunkel IKA-Laboratory, Staufen, Germany) in lysis solution [1% sodium dodecyl sulfate, Tris-HCl 10 mM, EDTA 50 mM, phenylmethylsulfonylfluoride 1 mM, aprotinin 1 μg/ml, and leupeptin 1 μg/ml (pH 7.4)] at 4 C for 10 min, transferred to Eppendorf tubes, and centrifuged at 20,800 $\times$ *g* at 4 C for 5 min. Proteins (100 μg) were separated by 12% SDS-PAGE and transferred to nitrocellulose. The membrane for measuring caspase 3 activation was incubated with anticaspase 3 rabbit polyclonal antibodies (Santa Cruz Biotechnology, Inc., Santa Cruz, CA) as primary antibodies and antirabbit-IgG-alkaline phosphatase (Sigma Chemical Co., St. Louis, MO) as secondary antibodies using 5-bromo-4-chloro-3-indolylphosphate p-toluidine salt and nitroblue tetrazolium chloride as alkaline phosphatase substrate.

Caspase 9 quantization followed the same procedure but using its specific antibody, anticaspase 9 (Santa Cruz Biotechnology).

Statistical analysis

Data are expressed as means ± SEM. Statistical significance was estimated with the paired or unpaired *t* test as appropriate. A *P* value less than 0.05 was considered significant. All analyses were performed using the SPSS version 10.0 (SPSS, Inc., Chicago, IL) statistical package.

Results

Characterization of mitochondrial dysfunction and the effect of low doses of IGF-I on parameters of mitochondrial function

MMP. The MMP, which is considered a good marker of mitochondrial function, was monitored by FL quenching of Rh-123 in mitochondria from the livers of rats under different conditions: the resting state 4 (with all substrates but ADP); the active state 3 (with ADP); and with oligomycin, which deactivates ATPase showing the conditions of maximum intramitochondrial negativity.

Table 1 summarizes the MMP values, expressed as arbitrary units (AU), in the three experimental groups. According to preliminary results (4), a reduction of MMP was observed in untreated aging rats compared with young controls, which IGF-I replacement therapy was able to restore to similar values to those found in young controls.

Mitochondrial oxygen consumption. Table 2 shows oxygen consumption under different conditions and RCRs in mitochondria from the three experimental groups.

O group showed higher values of oxygen consumption compared with young controls, but no significant differences were found between yCO and O + IGF-I groups. Interestingly, mitochondria from old rats treated with IGF-I expended significantly lower amounts of oxygen compared with O group ($P < 0.05$) with a significantly better efficiency because MMP returned to values similar to those found in young controls, whereas O showed a depletion of MMP as is described in Table 1 and in a preliminary study (4).

In addition, the ratio ADP to O expressing oxidative phosphorylation as ATP produced by oxygen molecule consumed, was significantly reduced in mitochondria from O group ($P < 0.05$ *vs.* yCO and O + IGF-I groups), whereas old

Downloaded from endo.endojournals.org at Univ San Pablo Biblioteca De Ciencias on March 10, 2009

TABLE 1. MMP (expressed as AU of FL) in isolated liver mitochondria with different substrates from the three experimental groups

	yCO group (n = 6)	O group (n = 6)	O + IGF-I group (n = 6)
Succinate (AU)	202 ± 19	169 ± 17[a]	199 ± 19[b]
+ ADP (AU)	141 ± 14	132 ± 18	141 ± 15
+ Oligomycin (AU)	229 ± 18	167 ± 18[a]	216 ± 10[b]
Glutamate/malate (AU)	175 ± 17	179 ± 12	169 ± 12
+ ADP (AU)	138 ± 17	140 ± 12	139 ± 11

Values are mean ± SEM. *P*, ns yCO group *vs.* O + IGF-I group in all conditions.
[a] $P < 0.05$ *vs.* yCO group.
[b] $P < 0.05$ *vs.* O group.

rats treated with low doses of IGF-I showed similar values to those found in young controls.

No significant differences were found among the three experimental groups in RCRs (state 3 to state 4).

Proton leak rates. The rate of proton leak across the inner mitochondrial membrane is a function of the driving force (membrane potential) and increases disproportionately with membrane potential (18–21). Proton leak rates express proton "escape" into mitochondrial matrix contributing to dissipation of the MMP in pathological conditions.

Figure 1 summarizes proton leak curves in the three experimental groups, expressed by oxygen consumption ($nAgO/mg{\cdot}min^{-1}$) at a given MMP in state 4 (without ADP). Mitochondria from O needed to consume increased oxygen compared with young controls to reach the same MMP values. Figure 1 showed that the proton leak curve of mitochondria from old animals treated with IGF-I was similar to the curve corresponding to young controls.

Activities of cytochrome oxidase and ATPase complexes. Cytochrome oxidase activity ($nAg\ O \times mg^{-1} \times min^{-1}$) expressed as oxygen consumption in this complex was significantly reduced in O group compared with young controls (yCO: 68.90 ± 4.60 *vs.* O: 48.40 ± 7.50; $P < 0.05$). However, no differences were found between yCO group and old rats treated with IGF-I [O + IGF-I: 62.33 ± 3.60, P = not significant (ns) *vs.* yCO and $P < 0.05$ *vs.* O group].

As shown in Fig. 2, ATPase activity (expressed as μmol ATP per mg protein) was significantly reduced in untreated aging rats. However, there were no significant differences between yCO and O + IGF-I groups in complex V activity, according to preliminary data (4).

Intramitochondrial free radical production. Figure 3 shows the intramitochondrial ROS production in isolated mitochondria from the three experimental groups in complex I (Fig. 3 A) using glutamate/malate as substrates and complex III (Fig. 3 B) with succinate plus antimycin as substrates. In both places, mitochondria from untreated aging rats showed a significant increase of ROS generation compared with mitochondria from young controls and O + IGF-I.

Blockage of oxygen consumption by Atr. In physiological conditions Atr is able to compete with ADP in ANT blocking mitochondrial respiration. As shown Fig. 4, Atr blocked oxygen consumption in mitochondria from young controls showing a normal inhibition of ANT. Full inhibition of the oxygen consumption induced by addition of ADP was obtained in liver mitochondria from young controls at a concentration of 150 pmol/mg Atr.

Peroxidation of ANT-thiol groups causes an uncoupling of ANT (28, 29). In this condition of oxidative damage, mitochondrial respiration is Atr insensitive. Thus, in this study Atr did not inhibit respiration in mitochondria from untreated aging rats (O group) (Fig 4). Interestingly, Atr inhibition was similar to young controls in mitochondria from O + IGF-I showing a normal inhibition of ANT. In this group (O + IGF-I) as shown in Fig. 4, full inhibition of the oxygen consumption induced by addition of ADP was obtained at a concentration of 200 pmol/mg Atr.

TABLE 2. Mitochondrial oxygen consumption by mitochondria from the three experimental groups

	yCO group (n = 6)	O group (n = 6)	O + IGF-I group (n = 6)
Glutamate/malate			
State 4 ($nAgO/mg{\cdot}min^{-1}$)	12.00 ± 1.00	14.00 ± 2.00	9.00 ± 1.00
State 3 ($nAgO/mg{\cdot}min^{-1}$)	43.00 ± 15.00	51.00 ± 17.00	30.00 ± 9.0[b]
RCR	3.60 ± 1.00	3.80 ± 1.50	3.00 ± 0.50
ADP/O	2.44 ± 0.24	1.51 ± 0.48[a]	2.46 ± 0.60[b]
Succinate			
State 4 ($nAgO/mg{\cdot}min^{-1}$)	29.00 ± 3.00	21.00 ± 2.00	18.00 ± 2.00[a]
State 3 ($nAgO/mg{\cdot}min^{-1}$)	93.00 ± 7.00	66.00 ± 6.00	70.00 ± 10.00
RCR	3.50 ± 1.00	3.00 ± 0.70	3.30 ± 0.80
ADP/O	1.80 ± 0.20	1.11 ± 0.30[a]	1.80 ± 0.30[b]

Values are mean ± SEM. ADP/O expresses oxidative phosphorylation: ATP produced by oxygen molecule consumed.
[a] $P < 0.05$ *vs.* yCO group.
[b] $P < 0.05$ *vs.* O group.

Downloaded from endo.endojournals.org at Univ San Pablo Biblioteca De Ciencias on March 10, 2009

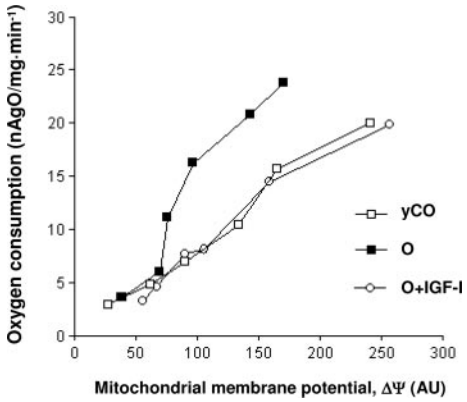

FIG. 1. Proton leak curves expressed by oxygen consumption (nAgO/mg·min^{-1}) by MMP in state 4 (without ADP). Proton leak rates express proton "escape" into mitochondrial matrix contributing to the dissipation of the MMP under pathological conditions. Mitochondria from O needed to consume an increased oxygen compared with young controls and old rats treated with IGF-I to reach the same values of MMP.

Mitochondrial oxidative damage, TAS, and intramitochondrial antioxidant enzyme activities in isolated liver mitochondria

Table 3 summarizes intramitochondrial oxidative damage, using LOOHs as markers, and total antioxidant capability of isolated mitochondria (26, 27) as well as the activities of mitochondrial antioxidant enzymes.

Mitochondria from O group showed an increase in oxidative damage and a reduction in TAS compared with young controls. IGF-I replacement therapy was able to improve both parameters.

However, GSHPx activity was significantly increased in both groups of old rats. In contrast, SOD activity was reduced in old rats, particularly in mitochondria from old rats treated with IGF-I. No significant differences were found between groups in GRD activity.

Measurements of caspase 3 and caspase 9 activation. Western blot for fragment 17 of caspase 3 showed a significant increase of caspase 3 activation in untreated aging rats compared with young controls (Fig. 5). However, a notable reduction in the expression of the active fragment of caspase 3 was observed in old animals treated with IGF-I.

Western blot for caspase 9 showed the same pattern with an increased expression in untreated aging rats compared with young controls (Fig. 5; $P < 0.06$). Again, IGF-I treatment induced a significant reduction of this parameter in old rats.

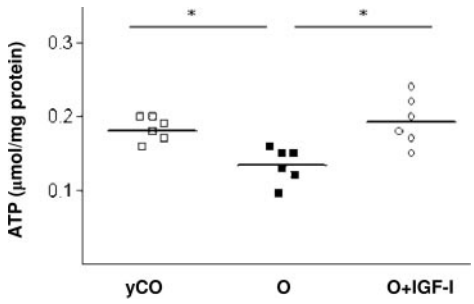

FIG. 2. Complex V, ATPase activity. ATPase activity was significantly reduced in mitochondria from untreated aging rats compared with young controls ($P < 0.05$) IGF therapy induced an increase of ATPase activity (P = ns *vs*. yCO group).

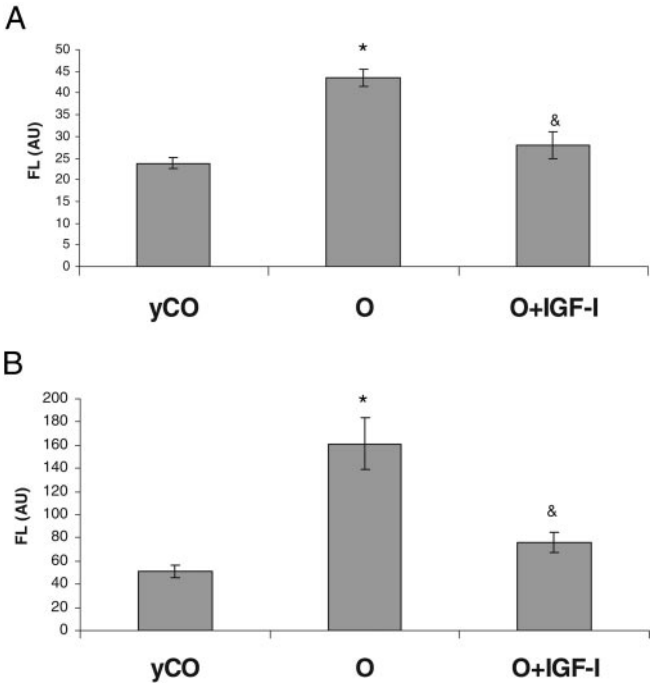

FIG. 3. Intramitochondrial free radical production (H_2O_2) in isolated mitochondria from the three experimental groups. A, Employing glutamate/malate as substrate (complex I). B, Employing succinate + antimycin as substrate (complex III). *, $P < 0.05$ *vs* yCO; &, $P < 0.05$ *vs* O; P = ns yCO *vs* O + IGF-I.

Discussion

Serum IGF-I levels decline with age (2, 3). Attending to our experience in liver cirrhosis (7–12), as a condition of IGF-I deficiency, we hypothesized that aging could be considered as a novel condition of IGF-I deficiency because circulating levels of this hormone are reduced, anabolism is diminished, and oxidative stress is one of the most important mechanisms of cellular damage in aging (2, 3, 27).

In fact, the administration of low doses of IGF-I restored IGF-I circulating levels, and were able to exert many beneficial effects on age related-changes improving testosterone levels, insulin resistance, lipid metabolism, and oxidative damage on brain and liver (4). We suggested that the described cytoprotection (neuroprotection and hepatoprotection) induced by IGF-I replacement therapy could be related to mitochondrial protection mechanisms. Thus, the present study was designed to analyze the effect of IGF-I on mitochondrial function leading to cellular protection. The mechanisms of IGF-I action are not completely understood, but data in this paper give some insight.

Compared with healthy young controls, untreated aging rats showed an increase of mitochondrial oxidative damage with a mitochondrial dysfunction characterized by depletion of membrane potential with increased proton leak and intramitochondrial free radical production, and a significant reduction of ATPase activity. In addition, mitochondrial respiration from untreated aging rats was Atr insensitive, show-

Downloaded from endo.endojournals.org at Univ San Pablo Biblioteca De Ciencias on March 10, 2009

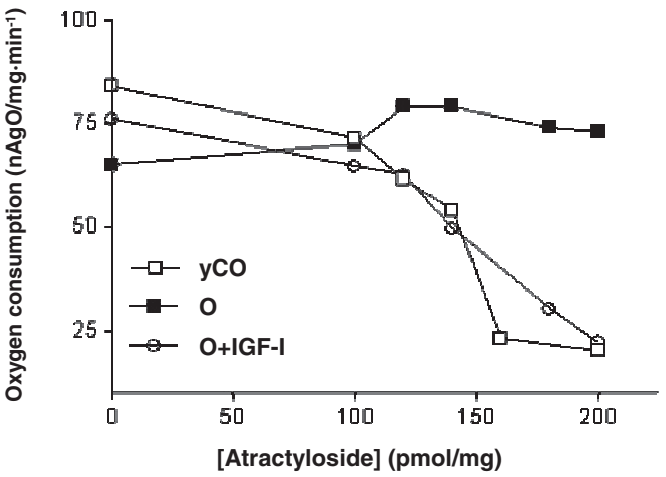

FIG. 4. Blockage of oxygen consumption by Atr. Mitochondria from untreated aging rats did not present an oxygen consumption blockage by Atr, suggesting an uncoupling of the ANT probably caused by peroxidation of ANT-thiol groups (28, 29). In this condition of mitochondrial oxidative damage (Table 3), respiration is Atr insensitive (n = 6 per group).

ing that ANT was uncoupled, probably due to peroxidation of thiol groups (28, 29). ANT has been shown to be one of the most sensitive places for pore opening. Consistent with these results, untreated aging rats showed a significant overexpression of the active fragment of caspase 3 and caspase 9. All of these findings contribute to characterize better the mitochondrial dysfunction associated with aging in this experimental model in rats. Results in this paper are in agreement with a significant amount of evidence that considers oxidative damage as one of the predominant mechanisms of cellular and tissular damage in aging. The ensuing oxidative stress leads to lipid peroxidation, mitochondrial dysfunction, and depletion of ATP (13, 27, 30–33). In aging, the selectively diminished activities of complexes I and IV have also been reported (32). In addition, it has been described that the ratio of ATP over oxygen consumed is reduced in aging, and this is associated with insulin resistance (31). Accordingly, we have recently reported that aging rats with mitochondrial dysfunction showed insulin resistance (4).

The major finding of this work was that mitochondrial dysfunction leading to apoptosis (activation of caspases) was improved by IGF-I therapy. In fact, IGF-I replacement therapy normalized mitochondrial oxidative damage and mitochondrial function (MMP and ATP synthesis), reducing intramitochondrial free radical generation, proton leak rates, and the vulnerability for pore opening in ANT, which was associated with a reduction of caspase 3 and 9 activation compared with O group.

The observed reduction of MMP with an increased generation of free radicals in aging rats suggests that oxygen is wasted by damaged mitochondria producing H_2O_2 instead of a normal proton gradient, the driving force of ATP synthesis through the proton pumping F_1F_0 ATP synthase (ATP synthase). In addition, proton leak rates were altered in aging rats. The rate of proton leak across the inner mitochondrial membrane increases disproportionately with membrane potential (13). Recently, ANT has been a significant mediator of the basal proton leak in mitochondria (21). In damaged mitochondria, peroxidation of ANT (or uncoupling proteins) facilitates the escape of protons into the mitochondrial matrix contributing to the MMP dissipation (16, 18–20).

Another point that deserves particular mention is that ANT has been one of the most sensitive places for mitochondrial pore opening (16, 34) for the release of cytochrome *c* activating caspases in cytosol (23). ANT contains a thiol group of a cysteine residues (Cys56) that are easily oxidized by ROS (16). In physiological conditions, Atr is able to compete with ADP in ANT blocking mitochondrial respiration. As was shown in Fig. 4, Atr blocked oxygen consumption induced by the addition of ADP in mitochondria from young controls showing a normal inhibition of ANT. Peroxidation of ANT-thiol groups causes an uncoupling of ANT. In this condition of oxidative mitochondrial damage, respiration is Atr insensitive. Thus, in this study Atr did not inhibit respiration in mitochondria from untreated aging rats (Fig. 4). This result is in agreement with other authors who have reported that aging enhances the activation of the permeability transition pore in mitochondria (34).

Of interest in the present work, IGF-I therapy reduced oxidative mitochondrial damage, correcting all these parameters of mitochondrial dysfunction, and resulting in a reduction of caspase 3 and 9 activation compared with O group. Together, these data suggest an extramitochondrial protection of mitochondria, which is not fully understood. Previously, we reported that low doses of IGF-I restored the expression of several protease inhibitors such us α-1-antichymotripsin, the serine protease inhibitor 2 in cirrhotic rats (35), which could contribute to the described mitochondrial protection. In agreement with these results, it has been re-

TABLE 3. Mitochondrial oxidative damage, and TAS and intramitochondrial antioxidant enzyme activities in isolated liver mitochondria from the three experimental groups

	yCO group	O group	O + IGF-I group
LOOH (nmol/mg mitochondrial prot)	1.00 ± 0.10	1.60 ± 0.05[a]	1.00 ± 0.15[b]
TAS (nmol/mg mitochondrial prot)	0.76 ± 0.08	0.53 ± 0.03[a]	0.69 ± 0.04
GSHPx (U/mg mitochondrial prot)	1.09 ± 0.14	2.55 ± 0.53[c]	2.16 ± 0.19[a]
SOD (U/mg mitochondrial prot)	5.76 ± 0.49	4.20 ± 0.33	2.86 ± 0.40[b,d]
GRD (U/mg mitochondrial prot)	47.99 ± 2.65	50.57 ± 5.51	43.67 ± 4.29

Values are mean ± SEM. prot, Protein.
[a] $P < 0.05$ *vs.* yCO.
[b] $P < 0.05$ *vs.* O.
[c] $P < 0.01$ *vs.* yCO.
[d] $P < 0.001$ *vs.* yCO.

Downloaded from endo.endojournals.org at Univ San Pablo Biblioteca De Ciencias on March 10, 2009

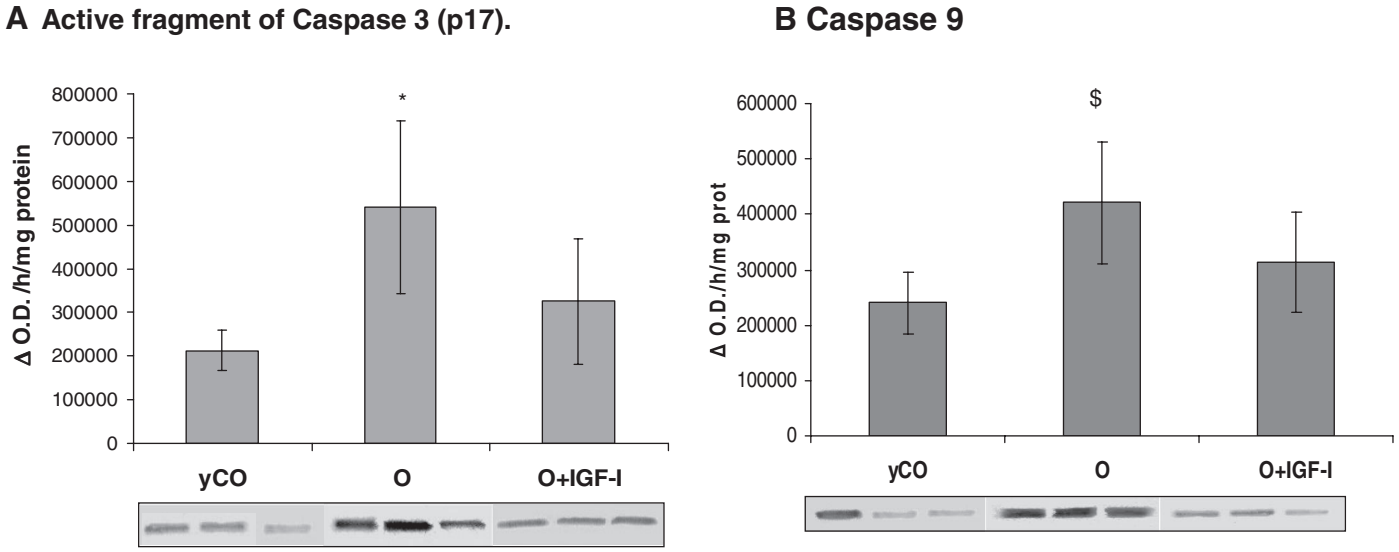

FIG. 5. Caspase activations by Western blot. Expression of the active fragment of caspase 3 (A) and caspase 9 (B). A, *, $P < 0.05$ *vs.* yCO; P = ns yCO *vs.* O + IGF-I. B, $, $P < 0.06$ *vs.* yCO; P = ns yCO *vs.* O+ IGF-I.

ported that IGF-I differentially regulates Bcl-xL and Bax, and confers myocardial protection in the rat heart (36).

In recent years, mitochondria have been recognized as regulators of cell death (13, 15, 22, 23). Intracellular or extracellular insults converge on mitochondria, inducing the so-called MMPT. The MMPT is an endpoint to initiate cell death and a putative target for cellular protection because MMPT and the release of mitochondrial cytochrome *c* activate the apoptotic pathway by which initiator caspases (*i.e.* caspases 8 and 9) are converted to their active forms, which in turn activate downstream effector caspases (*i.e.* caspases 3, 6, and 7) (15). Finally, cellular targets of the effector caspases include endonucleases and cytoskeletal proteins (13, 15).

These results show that IGF-I induces cell resistance to apoptosis by oxidative stress through mitochondrial protection. Mitochondria seem to be one of the most important cellular targets of IGF-I actions. Likewise, our data are in agreement with the observation that the effect of serum withdrawal on the autophagy of dysfunctional mitochondria is prevented by the addition of IGF-I (34). Accordingly, it has been reported that IGF-I inhibited the reduction of MMP, cytochrome *c* release, caspase 3 activity, and apoptosis in several cell lines and experimental procedures (38–41).

The described improvement of mitochondrial function in aging rats by IGF-I therapy resulted in an increment of ATP synthesis. Interestingly, several beneficial metabolic effects of IGF-I in aging (4) could be related to an increment of ATP availability after IGF-I therapy.

In conclusion, results in this paper show that the cytoprotective effect of IGF-I is closely related to a mitochondrial protection, leading to the reduction of intramitochondrial free radical production, oxidative damage, and apoptosis, and to increased ATP production. This work provides new evidence of the beneficial effect of IGF-I replacement therapy in aging.

Acknowledgments

We thank Dr. Bruce Scharschmidt, Chiron Company (Emeryville, CA), for granting the recombinant human IGF-I used in this study. We also thank Ms. Yolanda Rico and Mr. Brian Crilly for their generous help.

Received November 13, 2007. Accepted February 6, 2008.

Address all correspondence and requests for reprints to: Inma Castilla Cortazar, M.D., Department of Medical Physiology, School of Medicine, University CEU-Universidad San Pablo, Boadilla del Monte, 28668, Madrid, Spain. E-mail: iccortazar@uma.es.

Disclosure Statement: The authors have nothing to disclose.

References

1. **Sara VR, Hall K** 1990 Insulin-like growth factors and their binding proteins. Physiol Rev 70:591–613
2. **Veldhuis JD, Liem AY, South S, Weltman A, Weltman J, Clemmons DA, Abbott R, Mulligan T, Johnson ML, Pincus S, Straume M, Iranmanesh A** 1995 Differential impact of age, sex steroid hormones, and obesity on basal versus pulsatile growth hormone secretion in men as assessed in an ultrasensitive chemiluminescence assay. J Clin Endocrinol Metab 80:3209–3222
3. **Ceda GP, Dall'Aglio E, Maggio M, Lauretani F, Bandinelli S, Falzoi C, Grimaldi W, Ceresini G, Corradi F, Ferrucci L, Valenti G, Hoffman AR** 2005 Clinical implications of the reduced activity of the GH-IGF-I axis in older men. J Endocrinol Invest 28:96–100
4. **García-Fernández M, Delgado G, Puche JE, González-Barón S, Castilla-Cortázar I** 2007 10 January Low doses of insulin-like growth factor I improve insulin resistance, lipid metabolism and oxidative damage in aging rats. Endocrinology [Epub ahead of print]
5. **Laron Z** 1996 Short stature due to genetic defects affecting growth hormone activity. N Engl J Med 334:463–465
6. **Wu A, Grant DB, Hambley J, Levi AJ** 1974 Reduced serum somatomedin activity in patients with chronic liver disease. Clin Sci Mol Med 47:359–366
7. **Castilla-Cortázar I, Prieto J, Urdaneta E, Pascual M, Nuñez M, Zudaire E, Prieto J** 1997 Impaired intestinal sugar transport in cirrhotic rats: correction by low doses of insulin-like growth factor I. Gastroenterology 113:1180–1187
8. **Castilla-Cortázar I, García M, Quiroga J, Diez N, Diez-Caballero F, Calvo A, Diaz M, Prieto J** 2000 Insulin-like growth factor I reverts testicular atrophy in rats with advanced liver cirrhosis. Hepatology 31:592–600
9. **Cemborain A, Castilla-Cortázar I, García M, Quiroga J, Muguerza B, Picardi A, Santidrian S, Prieto J** 1998 Osteopenia in rats with liver cirrhosis: beneficial effects of IGF-I-treatment. J Hepatol 28:122–131
10. **Castilla-Cortázar I, García M, Muguerza B, Perez R, Quiroga J, Santidrián S, Prieto J** 1997 Hepatoprotective effects of insulin-like growth factor I in rats with carbon tetrachloride-induced cirrhosis. Gastroenterology 113:1682–1691
11. **Muguerza B, Castilla-Cortazar I, Garcia M, Quiroga J, Santidrian S, Prieto J** 2001 Antifibrogenic effect in vivo of low doses of insulin-like growth factor-I in cirrhotic rats. Biochim Biophys Acta 1536:185–195

Downloaded from endo.endojournals.org at Univ San Pablo Biblioteca De Ciencias on March 10, 2009

12. **Pérez R, García-Fernández M, Castilla-Cortázar I, Quiroga J, Delgado G, González-Barón S, Prieto J** 2001 Effect of IGF-I on mitochondrial dysfunction in rats with carbon tetrachloride-induced cirrhosis. J Hepatol 34:79
13. **Kowaltowski AJ, Vercesi E** 1999 Mitochondrial damage induced by conditions of oxidative stress. Free Radic Biol Med 26:463–471
14. **Cardoso SM, Pereira C, Oliveira CR** 1999 Mitochondrial function is differentially affected upon oxidative stress. Free Radic Biol Med 26:3–13
15. **Earnshaw WC, Martins LM, Kaufmann SH** 1999 Mammalian caspases: structure, activation, substrates, and functions during apoptosis. Annu Rev Biochem 68:383–424
16. **Brand MD, Pakay JL, Ocloo A, Kokoszka J, Wallace DC, Brookes PS, Cornwall EJ** 2005 The basal proton conductance of mitochondria depends on adenine nucleotide translocase content. Biochem J 392(Pt 2):353–362
17. **O'Connor JE, Vargas JL, Kimler BF, Hernandez-Yago J, Grisolia S** 1988 Use of rhodamine 123 to investigate alterations in mitochondrial activity in isolated mouse liver mitochondria. Biochem Biophys Res Commun 151:568–573
18. **Brand MD** 1990 The proton leak across the mitochondrial inner membrane. Biochim Biophys Acta 1018:128–133
19. **Barger JL, Barnes BM, Boyer BB** 2006 Regulation of UCP1 and UCP3 in arctic ground squirrels and relation with mitochondrial proton leak. J Appl Physiol 101:339–347
20. **Brand MD** 1995 Measurement of mitochondrial proton motive force. In: Brown GC, Cooper CE, eds. Bioenergetics: a practical approach. Oxford, UK: Oxford University Press; 39–62
21. **Monemdjou S, Kozak LP, Harper ME** 1999 Mitochondrial proton leak in brown adipose tissue mitochondria of Ucp1-deficient mice is GDP insensitive. Am J Physiol 276(6 Pt 1):E1073–E1082
22. **Bras M, Queenan B, Susin SA** 2005 Programmed cell death via mitochondria: different modes of dying. Biochemistry (Mosc) 70:231–239
23. **Cortese JD, Voglino AL, Hackenbrock CR** 1994 Persistence of cytochrome c binding to membranes at physiological mitochondrial intermembrane space ionic strength. Biochim Biophys Acta 1228:216–228
24. **National Academy of Sciences** 1991 The guiding principles for research involving animals. Washington, DC: National Institutes of Health
25. **Arab K, Steghens JP** 2004 Plasma lipid hydroperoxides measurement by an automated xylenol orange method. Anal Biochem 325:158–163
26. **Miller NJ, Rice-Evans C, Davies MJ** 1993 A new method for measuring antioxidant activity. Biochem Soc Trans 21:95S
27. **Voss P, Siems W** 2006 Clinical oxidation parameters of aging. Free Radic Res 40:1339–1349
28. **Vieira HL, Haouzi D, El Hamel C, Jacotot E, Belzacq AS, Brenner C, Kroemer G** 2000 Permeabilization of the mitochondrial inner membrane during apoptosis: impact of the adenine nucleotide translocator. Cell Death Differ 7:1146–1154
29. **Halestrap AP, Woodfield KY, Connern CP** 1997 Oxidative stress, thiol reagents, and membrane potential modulate the mitochondrial permeability transition by affecting nucleotide binding to the adenine nucleotide translocase. J Biol Chem 272:3346–3354
30. **Navarro A, Boveris A** 2007 The mitochondrial energy transduction system and the aging process. Am J Physiol Cell Physiol 292:C670–C686
31. **Ritz P, Berrut G** 2005 Mitochondrial function, energy expenditure, aging and insulin resistance. Diabetes Metab 31:5S67–5S73
32. **Kwong LK, Sohal RS** 2000 Age-related changes in activities of mitochondrial electron transport complexes in various tissues of the mouse. Arch Biochem Biophys 373:16–22
33. **Cortopassi GA, Wong A** 1999 Mitochondria in organism aging and degeneration. Biochim Biophys Acta 1410:183–193
34. **Mather M, Rottenberg H** 2000 Aging enhances the activation of the permeability transition pore in mitochondria. Biochem Biophys Res Commun 273:603–608
35. **Mirpuri E, Garcia-Trevijano ER, Castilla-Cortazar I, Berasain C, Quiroga J, Rodriguez-Ortigosa C, Mato JM, Prieto J, Avila MA** 2002 Altered liver gene expression in CCl4-cirrhotic rats is partially normalized by insulin-like growth factor-I. Int J Biochem Cell Biol 34:242–252
36. **Yamamura T, Otani H, Nakao Y, Hattori R, Osako M, Imamura H** 2001 IGF-I differentially regulates Bcl-xL and Bax and confers myocardial protection in the rat heart. Am J Physiol Heart Circ Physiol 280:1191–1200
37. **Tsujimoto Y** 2003 Cell death regulation by the Bcl-2 protein family in the mitochondria. J Cell Physiol 195:158–167
38. **Gu Y, Wang C, Cohen A** 2004 Effect of IGF-1 on the balance between autophagy of dysfunctional mitochondria and apoptosis. FEBS Lett 577:357–360
39. **Leinninger GM, Russell JW, van Golen CM, Berent A, Feldman EL** 2004 Insulin-like growth factor-I regulates glucose-induced mitochondrial depolarization and apoptosis in human neuroblastoma. Cell Death Differ 11:885–896
40. **Kondo T, Kitano T, Iwai K, Watanabe M, Taguchi Y, Yabu T, Umehara H, Domae N, Uchiyama T, Okazaki T** 2002 Control of ceramide-induced apoptosis by IGF-1: involvement of PI-3 kinase, caspase-3 and catalase. Cell Death Differ 9:682–692
41. **Ness JK, Scaduto RC, Wood TL** 2004 IGF-I prevents glutamate-mediated bax translocation and cytochrome c release in O4+ oligodendrocyte progenitors. Glia 46:183–94
42. **Schneider WC, Hogeboom GH** 1950 Intracellular distribution of succinoxidase and cytochrome oxidase activities in normal mouse liver and in mouse hepatoma. J Natl Cancer Inst 10:969–975

***Endocrinology* is published monthly by The Endocrine Society (http://www.endo-society.org), the foremost professional society serving the endocrine community.**

Downloaded from endo.endojournals.org at Univ San Pablo Biblioteca De Ciencias on March 10, 2009